4ICEGE
Thessaloniki-GREECE 2007

4th International Conference on
Earthquake Geotechnical Engineering
June 25-28, 2007
Paper No. 1583

ZONE OF EXCESSIVE GROUND SURFACE DISTORTION DUE TO DIP-SLIP FAULT RUPTURE

Achilleas PAPADIMITRIOU [1] , Dimitrios LOUKIDIS [2]
George BOUCKOVALAS [3] , Dimitrios KARAMITROS [4]

ABSTRACT

This paper studies the zone of excessive ground surface distortion created by a dip-slip active fault rupture propagating from the bedrock through a soil layer during an earthquake. The simulation of the fault rupture propagation through the soil layer is performed via quasi-static numerical analyses using the finite difference code *FLAC*. The analysis focuses on the geometry of the developing shear band and the distribution of surface displacements. The paper presents results from 28 parametric analyses that quantify the effects of soil type, fault type and fault dip angle in the bedrock. The results of the analyses are presented in the form of charts and equations for the rough prediction of the location and the width of the zone of significant surface distortion, and the estimation of the fault displacement required for the rupture to reach the ground surface. An example of the fault propagation prediction in an actual case is presented for the well documented rupture of the Nikomidino fault (Volvi basin in Northern Greece, 20-6-1978). In practice, these results can be used for the definition of zones where construction is disallowed (set-back limits) and of zones where damage-preventing countermeasures should be considered in the design of light-weight structures and lifelines (e.g. pipelines).

Keywords: fault rupture, microzonation, setback limits, lifelines, earthquake

INTRODUCTION

The design of structures in the vicinity of active faults is one of the most difficult problems of earthquake engineering. An indication of the complexity of the problem is that seismic codes generally require the execution of a specialized study for any structure, even though there is no specific methodology in the literature for performing such a study. Moreover, many seismic codes, including the Greek code EAK (2002), refer to a zone where construction is disallowed, but do not specifically define its width and location.

Additional difficulties arise when the active fault is buried under a soil layer of significant thickness (e.g. a few tens of meters). In such a case, even if the location (trace) and the characteristic of the fault in the geologic bedrock (type, dip angle β and expected displacement d) are well defined, there are three (3) practical questions that need to be answered:

a) Will the fault rupture reach the ground surface and at which location?
b) At which zone will the ground surface distortion be prohibitive for conventional construction?
c) Will the seismic motion be amplified in the vicinity of the fault and by which amount?

In this paper, the emphasis is set on answering the first two questions, since the third cannot be confidently answered without employing large scale seismological monitoring and interpretation. In

[1] Lecturer, Dept. of Civil Engineering, University of Thessaly, Greece, Email: apapad@civ.uth.gr
[2] Post-Doctoral Researcher, Dept. of Civil & Environmental Engineering, Purdue University, USA
[3] Professor, School of Civil Engineering, National Technical University of Athens, Greece
[4] PhD Candidate, School of Civil Engineering, National Technical University of Athens, Greece

this endeavor, researchers have employed various approaches: a) case studies (e.g. Lade et al 1984, Bray et al 1994a, Mercier et al 1983, Kelson et al 2001), b) experimental studies (e.g. small scale experiments by Cole and Lade 1984, centrifuge experiments by Roth et al 1981) and c) numerical studies (e.g. Roth et al 1982, Bray et al 1994). Attempting to generalize results from all different types of studies showed that there is a need for a systematic and combinatory analysis. This paper aims to contribute to this effort via numerical analyses that are in accordance with the findings from the literature.

NUMERICAL METHODOLOGY

The numerical simulations of the active fault rupture propagation through a soil layer are hereby performed using the finite difference code *FLAC* (Itasca Inc 1998). The emphasis is put on dip-slip (normal and reverse) faults and not on strike-slip faults whose rupture propagates almost vertically and is practically not affected by soil conditions (e.g. Bray et al 1994a).

Figure 1 presents the typical mesh and boundary conditions used in the foregoing analyses. For reasons of simplicity, the ground surface and the soil-bedrock interface are assumed horizontal, i.e. the soil layer is assumed horizontal and of uniform height *H*. The mesh discretization on top of the fault trace in the bedrock (central region of the mesh) is denser and consists of square elements (or "zones" in *FLAC* terminology) so as not to influence the mechanism of fault rupture propagation. Moreover, the ratio of the total mesh width to the mesh height is at least 4:1 in all analyses, so as to minimize the effects of the lateral mesh boundaries on the strain accumulation pattern in the central region of the mesh.

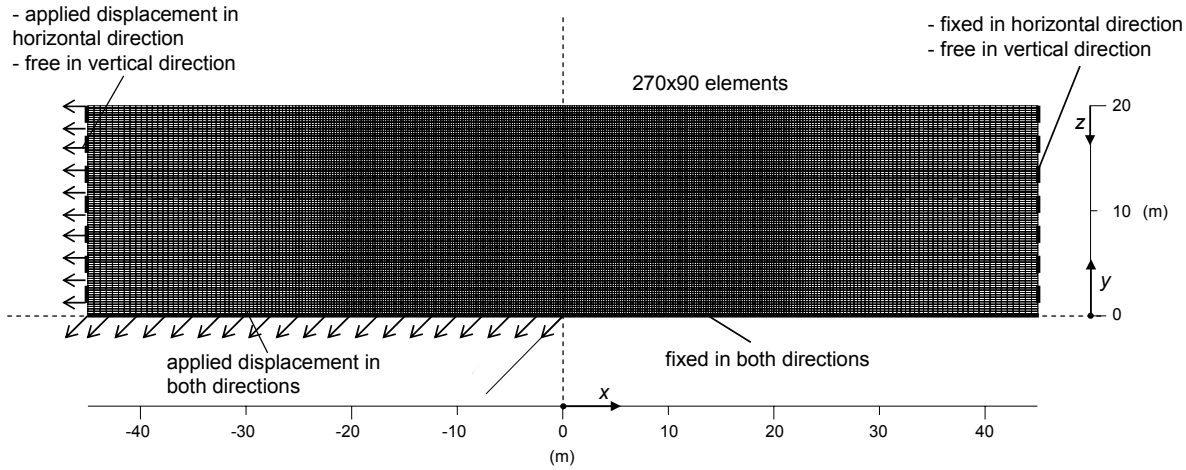

Figure 1. Typical mesh and boundary conditions of the numerical analyses

Displacement increments are prescribed at the segment of the soil-bedrock interface corresponding to the moving block. The lateral mesh boundaries have also prescribed horizontal displacement (non-zero for the moving block), but are allowed to move freely in the vertical direction. The prescribed displacements at the mesh boundaries depend on the simulated fault dip angle and are applied at a very low rate so as to minimize inertial effects. Hence, all the analyses performed in the context of this study are practically quasi-static. Given that the fault rupture propagation is governed by the soil behavior, not only at yield, but mainly in post-yield conditions, the non cohesive soil response was simulated with the use of a Mohr-Coulomb constitutive model that allows for strain softening. For cohesive soils, for which the rupture is propagated under undrained conditions, the same constitutive model was used, but the shear strength was defined on the basis of the undrained shear strength S_u.

VALIDATION OF NUMERICAL METHODOLOGY

The validation of the numerical methodology was performed via qualitative and quantitative comparison with results from the literature. For example, Figure 2 compares qualitatively the numerical results of Loukidis (1999) and Loukidis and Bouckovalas (2001) in terms of the shear strain rate contours for the case of a dense sand layer overlying a reverse fault with a dip angle $\beta = 135^o$ (or -45^o) to respective field observations. These results show that the propagating rupture bends towards the stationary block (foot wall). This is a general trend for reverse faults in the literature (e.g. Bray et al 1994). On the other hand, the rupture of normal faults generally bends towards the moving block (hanging wall).

(a)

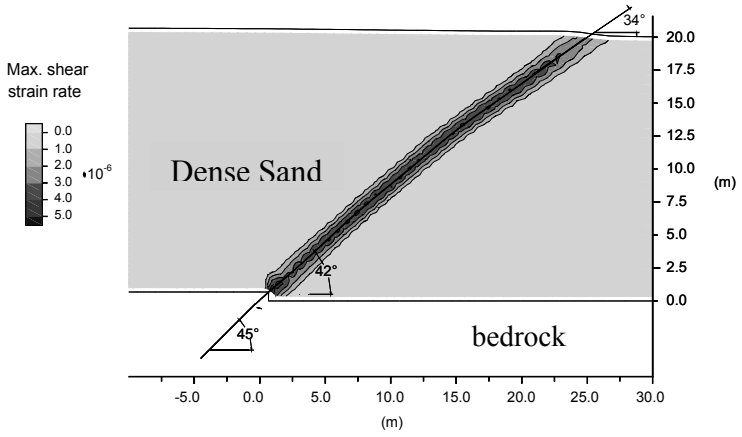

(b)

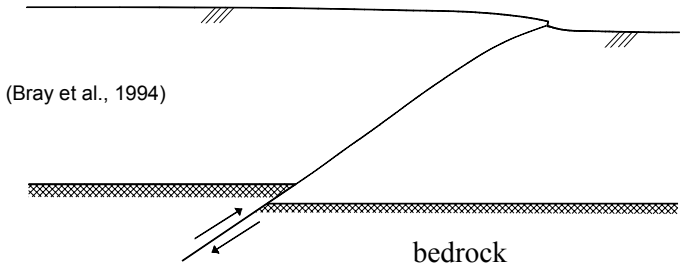

Figure 2. Depiction of failure surface from fault rupture propagation of a reverse dip-slip fault with β=135^o through dense sand: a) numerical results in terms of maximum shear strain rate contours (Loukidis 1999), b) related field evidence (Bray et al 1994)

For a quantitative evaluation of the methodology, the case of the 1978 Nikomidinon normal fault rupture was chosen. This is one of four normal faults in the Volvi basin and its rupture is associated with the great Thessaloniki (Northern Greece) earthquake (June 20th 1978). More specifically, during that earthquake the fault rupture in the bedrock propagated to the ground surface and its failure surface was studied in detail by Mercier et al (1983), as shown in Figure 3b. Based on detailed geological, geophysical and geotechnical data for the area (given its proximity to the Euroseistest Project test site, e.g. Raptakis et al 2000), a series of numerical analyses was performed (Antoniou 2000, Bouckovalas et al 2001) taking into account the local site conditions. Various indices can be used for the depiction of the failure surface within the soil layer. The clearest illustration of the failure surface width and curvature is achieved with the use of the shear strain rate contours, as shown by the comparison of the numerical results in Figure 3b to the field observations in Figure 3a.

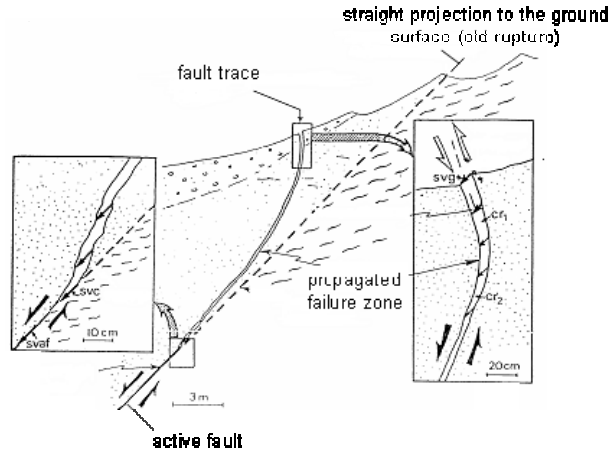

(a)

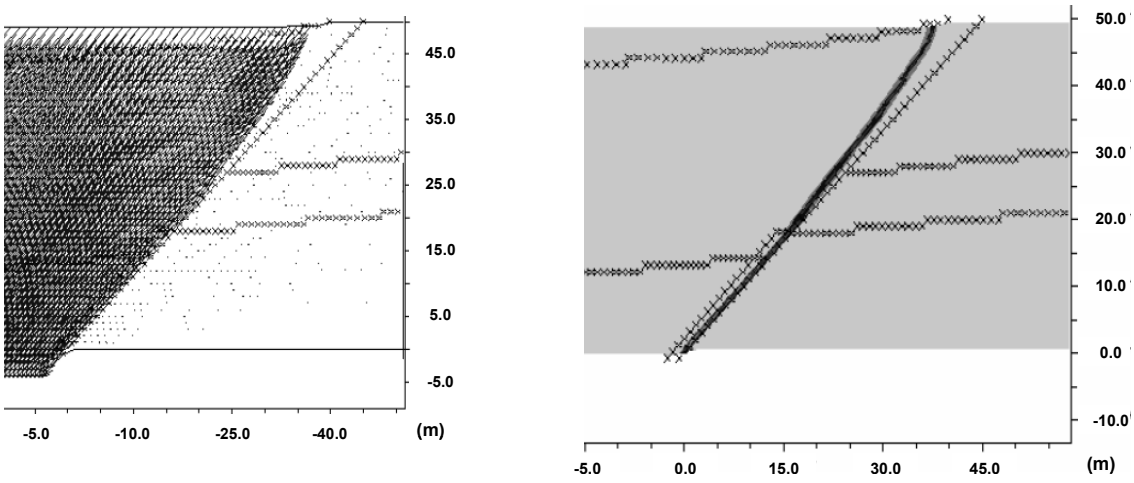

(b)

Figure 3. Depiction of failure surface of the 1978 Nikomidino normal fault rupture: a) field evidence (Mercier et al 1983), b) numerical simulation results (Antoniou 2000)

PARAMETRIC ANALYSES

Twenty eight (28) parametric analyses were performed for the study of the fault rupture propagation and the ground surface distortion, as a function of the dip angle β of the fault in bedrock, the fault displacement d and the type of the soil layer. Specifically, the analyses focused on seven (7) values of the dip angle of the fault in bedrock $\beta = 45^o$, 60^o, 75^o, 90^o, 105^o, 120^o and 135^o and four (4) soil types: Loose Sand (LS), Dense Sand (DS), Normally-consolidated Clay (NC) and Overconsolidated Clay (OC). Note that in terms of terminology, a fault is considered normal for dip angles $\beta = 45^o$, 60^o and 75^o, and reverse for $\beta = 105^o$, 120^o and 135^o, while a case of $\beta = 90^o$ is the borderline case of a vertical dip-slip fault. The soil layer thickness H in the aforementioned parametric runs was 20m. A limited number of analyses with H ranging from 5m to 80m were also carried out in order to assess the influence of the layer thickness.

Regarding the material properties of the Mohr-Coulomb constitutive model (Table 1):

- The Young's modulus E for the cohesive soils is assumed a linear function of the effective overburden stress (but also of the overconsolidation ratio OCR for the OC clays), while for non-cohesive soils it is assumed a function of $z^{1/2}$

Table 1. Material properties of the Mohr-Coulomb model used in the numerical simulations

Constant	LS	DS	NC	OC
ρ (t/m^3)	1.6	1.8	1.8	2.0
E (kPa)	$7910\sqrt{z}$	$11375\sqrt{z}$	$876z$	$1076z\left[0.8\left(1+\frac{1.5H}{z}\right)\right]^{0.8}$
v	0.333	0.333	0.460	0.495
c (kPa)	0	0	$2z$	$2z\left[0.8\left(1+\frac{1.5H}{z}\right)\right]^{0.8}$
t_c (kPa)	-	-	-	$z\left[0.8\left(1+\frac{1.5H}{z}\right)\right]^{0.8}$
φ_{max} (^{o})	30	45	0	0
φ_{res} (^{o})	-	30	-	-
ψ_{max} (^{o})	0	15	0	0
ψ_{res} (^{o})	-	0	-	-
γ_{res} (^{o})	-	10	-	-

- For the non-cohesive soils, the peak friction angle was set to φ_{max} = 30^o and 45^o for loose (LS) and dense sand (DS) respectively, while the peak dilatancy angle was set to ψ_{max} = 0^o and 10^o, respectively. The strain softening of the dense sand led to residual values of φ_{res}=30^o and ψ_{res}=0^o that are attained at a shear strain level of 10%.
- For the cohesive soils, the undrained shear strength for NC clay is given by S_u(NC) = $0.25\sigma'_{vo}$ with zero tensile strength t_c, whereas for the OC clay the S_u profile is given by S_u(OC) = S_u(NC)OCR$^{0.8}$, with a tensile strength t_c equal to S_u/2.

Figures 4, 5, 6 and 7 present the evolution of the ground surface distortion with increasing bedrock fault displacement d/H, for fault dip angles β = 45^o, 60^o, 75^o, 105^o, 120^o and 135^o and for all four (4) soil types LS, DS, NC and OC, respectively. The distorted ground surface is presented in terms of the displaced nodal coordinates (x and y), normalized in terms of the thickness H of the soil layer. Note that before the initiation of the fault rupture, the horizontal ground surface is at elevation y = 0 and that the fault trace in the bedrock is located at x = 0.

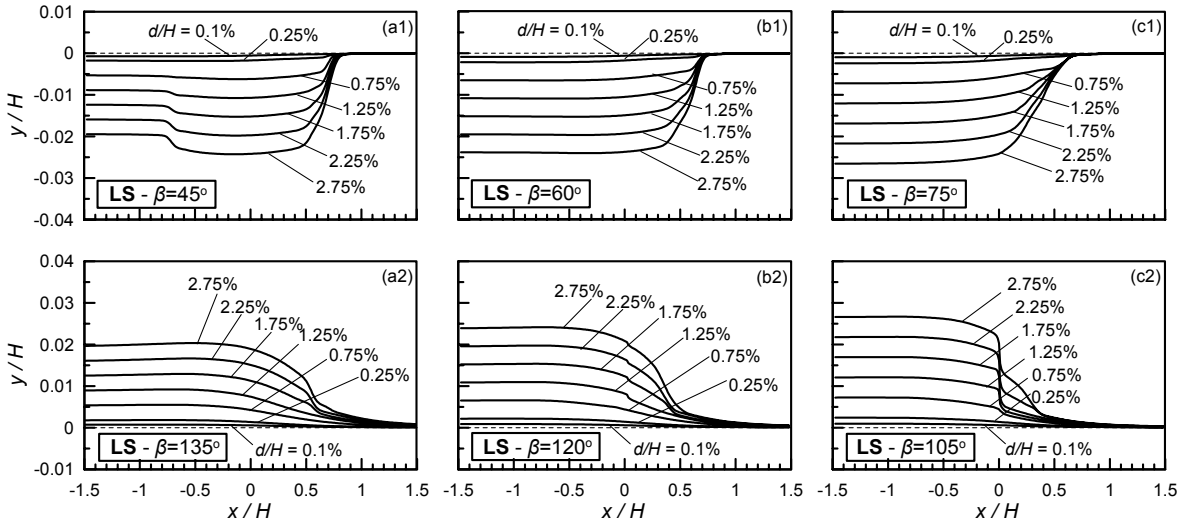

Figure 4. Ground surface distortion with increasing fault displacement *d/H*, for faults with different dip angles *β* underlying a layer of Loose Sand (LS)

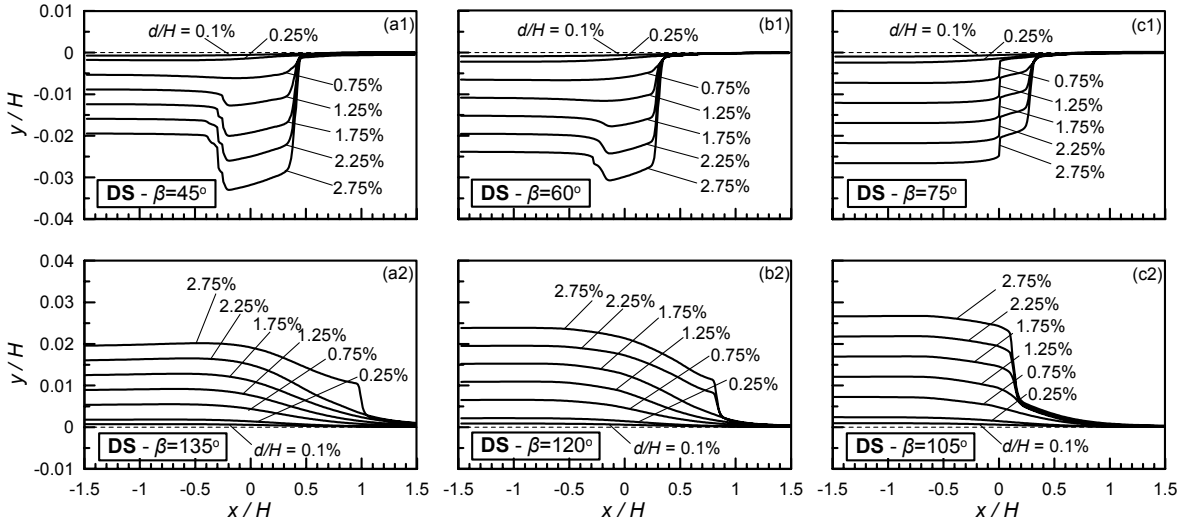

Figure 5. Ground surface distortion with increasing fault displacement *d/H*, for faults with different dip angles *β* underlying a layer of Dense Sand (DS)

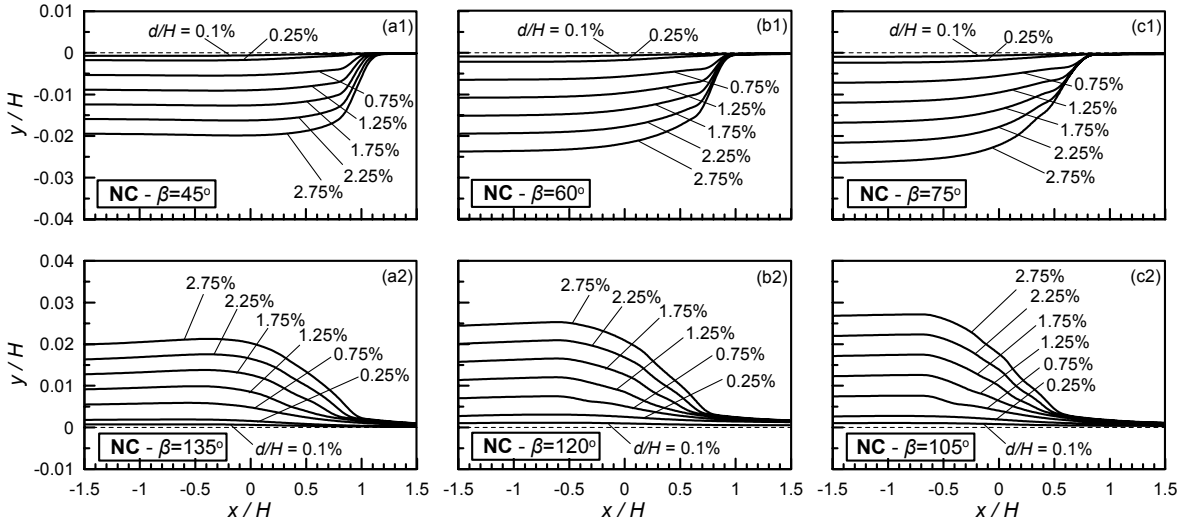

Figure 6. Ground surface distortion with increasing fault displacement *d/H*, for faults with different dip angles *β* underlying a layer of Normally-consolidated Clay (NC)

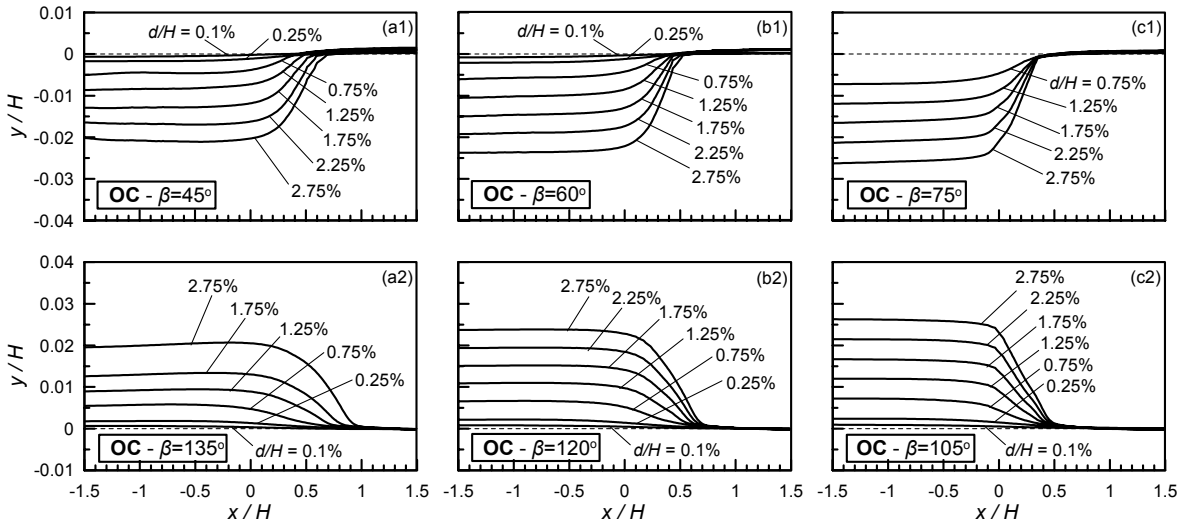

Figure 7. Ground surface distortion with increasing fault displacement *d/H*, for faults with different dip angles *β* underlying a layer of Overconsolidated Clay (OC)

The exact form of the distorted ground surface is of relatively small practical importance, for preliminary design purposes at least. More important is the knowledge of the value of specific parameters, like (see Figure 8):

a) the value of the bedrock fault displacement d_o/H for the rupture to reach the ground surface,

b) the width L of the zone with significant ground surface distortion, and

c) the location C of the foregoing zone with significant ground surface distortion,

which are the subjects of the next paragraphs.

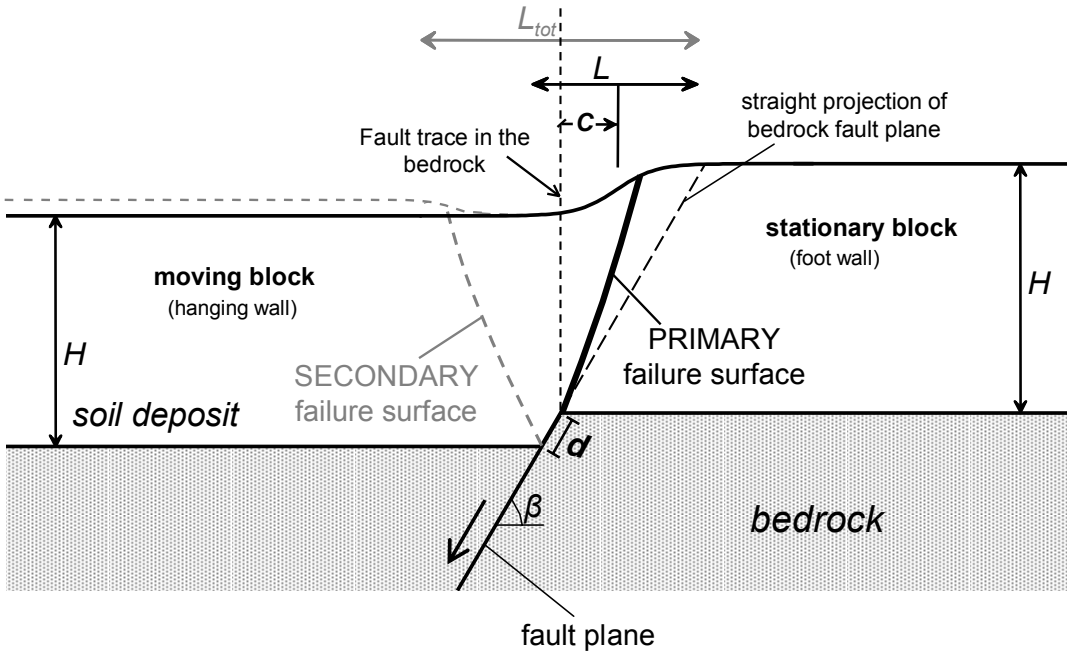

Figure 8. Schematic illustration of the problem of fault rupture propagation through soil layer and parameters of engineering interest

Fault displacement for the rupture to reach the ground surface

Numerical results show that an increase of the bedrock fault displacement d/H generally leads to an increase of the maximum inclination of the ground surface. This increase is characterized by a slow initial rate up until a limiting value of bedrock fault displacement d_o/H beyond which the maximum ground surface inclination increases intensely, a fact depicting that the rupture has reached the ground surface. This value of the limiting fault displacement is presented in Figure 9, as a function of the fault dip angle β and for all four (4) soil types considered here.

It is deduced that for normal faults, the rupture reaches the ground surface for much smaller bedrock fault displacements (d_o/H = 0.2 ÷ 0.4%) as compared to reverse faults (d_o/H = 0.3 ÷ 2.4%). One possible explanation for this difference is that reverse faulting occurs in a compressional stress regime oppositely to normal faulting that occurs in a tensile stress regime. This difference is reminiscent of the difference between passive and active failure conditions of retaining walls, which require similarly different strain levels in order to occur.

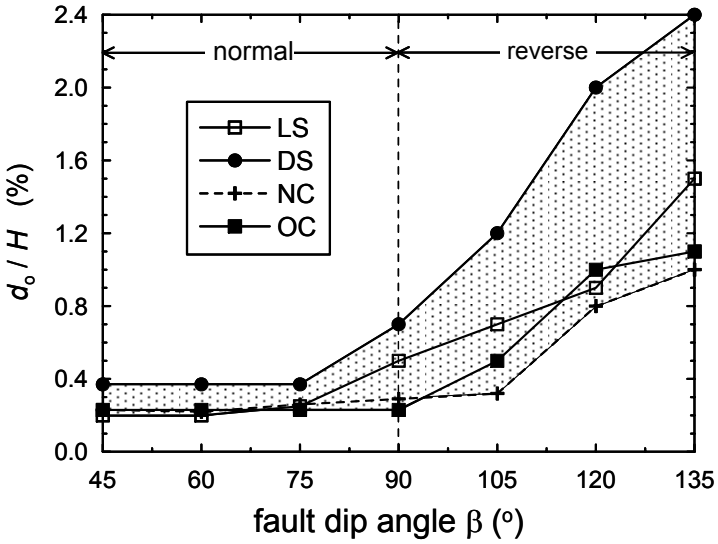

Figure 9. Minimum fault displacement d_o/H for the rupture to reach the ground surface

Width of zone with significant ground surface distortion

This study considers as zone of significant ground distortion the region where the ground surface inclination is larger than 1/500 or 0.2%. This limit was chosen since it is the traditional serviceability limit of angular distortion for shallow foundations with spread footings. Interestingly, the width L of this zone tends to remain practically constant for bedrock fault displacements $d/H > 1\%$. Hence, the width L normalized with respect to soil thickness H for all analyses is presented in Figure 10, as a function of the bedrock fault dip angle β and for the four (4) soil types considered here. Moreover, for the cases where a graben is formed, Figure 10 presents the total width L_{tot}/H of significant ground surface distortion which includes the width of the graben and the width of the distortion zone associated with the secondary rupture.

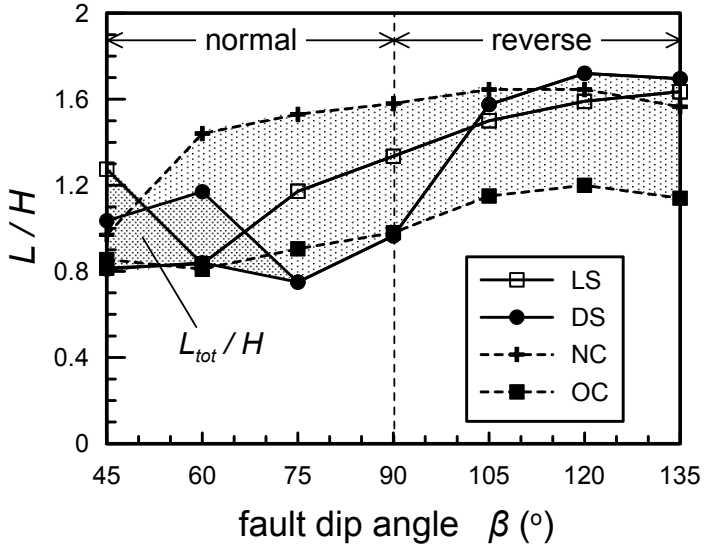

Figure 10. Normalized width L/H of zone with significant ground surface distortion

It is interesting to note that the present numerical results suggest that the higher the d_o/H is, the higher the L/H is expected to be (Figures 9 and 10), especially for non-cohesive soils (LS and DS). Given that, during the initial stages of bedrock fault movement, the zone of ground distortion increases with d/H, this trend implies that the width of the zone of significant ground distortion L/H is affected by the amount of deformation accumulated prior to the emergence of the fault rupture to the ground surface.

Hence, the fact that the width L/H for normal faults is generally smaller than that of reverse faults may be attributed to the relatively larger values of d_o/H in reverse fault cases (see Figure 9) and the aforementioned interrelation between d_o/H and L/H. Nevertheless, the difference in the values of L/H is not as large as the difference in the values of d_o/H, and this because the L/H practically ceases to develop at d/H >1%, in all cases, as mentioned above.

Location of zone of significant ground surface distortion

Using Figure 10 for practical applications (i.e. defining setback limits for construction of civil engineering works) requires locating the zone of significant ground surface distortion with respect to the fault trace in the bedrock. This positioning is performed here via C, i.e. the distance of the center of the foregoing zone (of width L) from the bedrock fault trace and towards the stationary block. Hence, Figure 11 summarizes the values of distance C, normalized with respect to thickness H, as a function of the bedrock fault dip angle β and for all four (4) soil types considered here.

It is deduced that the normalized location C/H is mostly a function of the bedrock fault dip angle β and less so of the soil type. Moreover, it is deduced that the center C/H of the zone of significant ground surface distortion rests between the fault trace in the bedrock (C/H = 0) and the straight projection of the bedrock fault plane to the ground surface (line denoted as "tan|90-β|"). For a vertical fault (β = 90°) in particular, C/H is practically zero, i.e. the zone of significant ground surface distortion is equally spaced on either side of the bedrock fault trace.

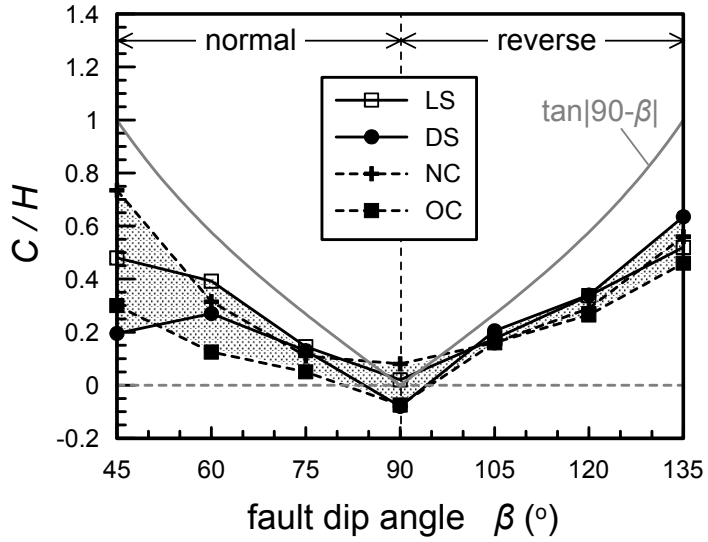

Figure 11. Normalized location of center of zone with significant ground surface distortion *C/H*

Effect of soil layer thickness *H*

All results in Figures 4 through 7 and 9 through 11 originate from analyses for which the soil layer thickness H is equal to 20m. Nevertheless, these results are plotted normalized over the soil layer thickness H, implying a generalization of their applicability for any value of H. In order to adopt this generalization, it is imperative to investigate its accuracy. In this respect, Figure 12 compares the values of L and d_o for various values of H ranging from 5m to 80m divided by their respective values for H = 20m. It is deduced that the generalization holds true for cohesive soils (NC and OC clays) and the results from the previous figures can be used safely without any need for a correction factor. This is not the case for non cohesive soils (LS and DS). In particular, Figure 12a shows that the normalized width L/H of the zone with significant ground surface distortion increases with increasing soil layer thickness H for non cohesive soils. However, the dependence of L/H on the soil cover thickness diminishes at large H values. The observed trend for non-cohesive soils (LS and DS) can be approximated by the following equation (Figure 12a):

$$\frac{L/H}{(L/H)_{20\mathrm{m}}} = \left(\frac{H(\mathrm{m})}{20}\right)^{0.12} \tag{1}$$

As shown in Figure 12b, the effect of the sand layer thickness H on the d_o/H for LS and DS is relatively stronger, and can be quantified with the aid of the following equation (Figure 12b):

$$\frac{d_o/H}{(d_o/H)_{20\mathrm{m}}} = \left(\frac{H(\mathrm{m})}{20}\right)^{0.4} \tag{2}$$

The above equations can be seen as correction factors to the respective data presented in previous subsections from the analyses with H = 20m. Based on Equations (1) and (2) when the bedrock fault displacement d_o/H increases so does the width L/H of non cohesive soils, but to a smaller degree. This interrelation of d_o/H and L/H for non-cohesive soils is reminiscent of what is observed in Figures 9 and 10 for normal and reverse faults. Focusing on the interpretation of the effect of H on the value of d_o/H, the following may be noted:

- The peak shear strength of both cohesive and non-cohesive soils are assumed linear functions of the vertical effective stress σ'_{vo} and thus of the depth z.
- The Young's modulus E of non-cohesive soils is assumed a non-linear function of the depth z (i.e. $z^{1/2}$). Therefore, self-similarity with respect to the elastic modulus profile does not hold for LA and DS, since E/H cannot be a function purely of the normalized depth z/H, oppositely to what happens in the case of NC and OC, based on the assumed soil properties shown in Table 1.

As a result, the yield strain (that is equal to the ratio of the shear strength divided by the elasticity modulus of the Mohr-Coulomb soil model) turns out to be independent of the depth z for cohesive soils and an increasing function of depth (i.e. $z^{1/2}$). Therefore, shallow non-cohesive deposits have a smaller yield strain as opposed to deep deposits, and as such they require relatively smaller values of d_o/H for the rupture to reach the ground surface (see Figure 12b). On the contrary, for cohesive deposits (NC and OC) the yield strain is independent of the soil depth and thus the d_o/H is proven independent of H (see Figure 12b). Given the interrelation of d_o/H and L/H, the relative increase (or decrease) of d_o/H leads to a smaller increase (or decrease) in the respective values of L/H.

For completeness it is noted that the effect of layer thickness H on the value of C/H is unimportant. An exception to this rule are the cases where a secondary rupture forms a graben, i.e. cases only possible when normal faults with low dip angles underlie non-cohesive soil.

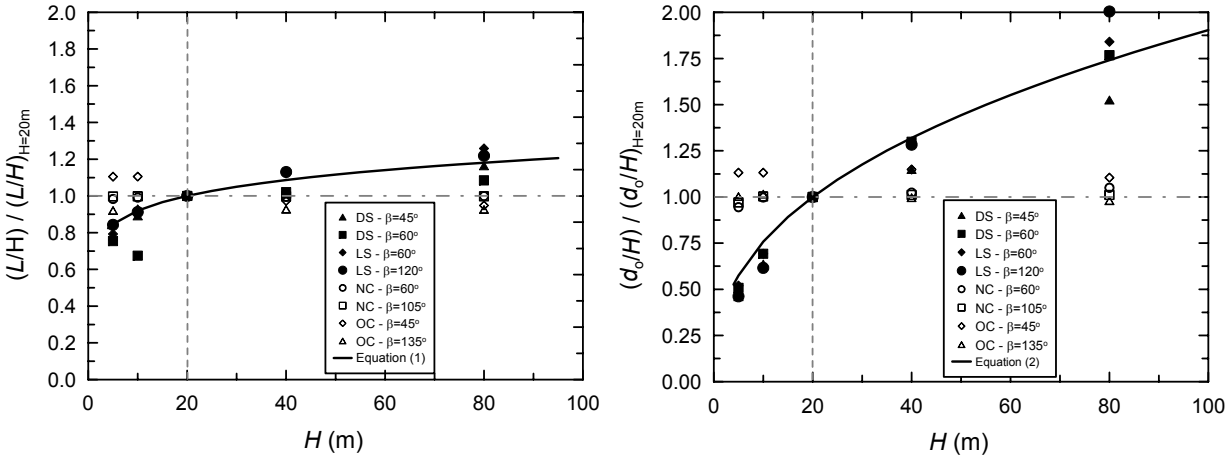

Figure 12. Effect of soil layer thickness H on a) the width L/H of the zone with significant ground surface distortion and b) the bedrock fault displacement d_o/H required for the rupture to reach the ground surface

CONCLUSIONS

The basic conclusions from this study are the following:

- The fault rupture propagation from the bedrock to the ground surface through a soil layer of thickness H may deviate significantly from the straight projection of the bedrock fault plane.
- For non-cohesive soils, the rupture propagation to the ground surface creates a scarp, whereas for cohesive soils the ground distorts more smoothly, with possible tension cracks in the case of OC clay. In particular, for non-cohesive soils and small normal fault dip angles β in the bedrock, a graben is formed in the ground.
- The bedrock fault displacement d_o required for the rupture to reach the ground surface and the location C and width L of the zone with significant ground surface distortion (i.e. where surface inclinations exceed 1/500 or 0.2%) are found to be a function of the soil thickness H and the dip angle β of the fault in the bedrock. The soil type has a relatively small effect on the values of C.
- In general, the width L of the zone with significant ground surface distortion ranges from $0.8H$ to $1.6H$, while the location C of the center of the foregoing zone is between the trace of the fault in the bedrock and its straight projection to the ground surface.
- The bedrock fault displacement required for the rupture to reach the ground surface is larger in the case of reverse faults (d_o/H = 0.3 – 2.4%) than in the case of normal faults (d_o/H = 0.2 – 0.4%).

The values of d_o, C and L can be estimated via charts and equations that are based on the results of this study. Use of these in practice presupposes the knowledge of the location, the dip angle and the expected displacement of the active fault in the bedrock, all objects of a seismo-tectonic study. In such a case, these charts can be used in seismic microzonation studies for the preliminary definition of zones of disallowed construction (set-back limits), as well as of zones where damage-preventing countermeasures should be considered in the design of light-weight structures and lifelines (e.g. pipelines). In all cases, these charts should be used parametrically for various possible locations of the fault in the bedrock, in cooperation with seismologists. On the other hand, these results cannot be used in the case of heavy structures, since the fault-soil-structure interaction may alter the location of the fault rupture at the ground surface.

Despite the qualitative and quantitative verification of the employed methodology, the fact that the proposed charts and equations stem from numerical analyses presents a need for further verification, with insitu and/or laboratory (preferably centrifuge) measurements. This process is currently under way. In all cases, it must be underlined that the studied problem is extremely complicated and poly-parametric and hence it is premature to consider general design criteria in the form of code provisions.

ACKNOWLEDGEMENTS

This research was partly funded from the project entitled “EPEAEK2 – Pythagoras” that is co-funded by the European Union and the Ministry of National Education and Religious Affairs of Greece.

REFERENCES

Antoniou K, “Numerical simulation of the Nikomidino fault rupture”, Diploma Thesis, Geotechnical Department, N.T.U.A., 2000 (in Greek)

Bray JD, Seed RB, Cluff LS and Seed HB, “Earthquake Fault Rupture Propagation through Soil”, Journal of Geotechnical Engineering, ASCE, 120 (3), 543-561, 1994a

Bray JD, Seed RB and Seed HB, “Analysis of Earthquake Fault Propagation through Cohesive Soil”, Journal of Geotechnical Engineering, ASCE, 120 (3), 562-580, 1994b

Bouckovalas GD, Loukidis D and Antoniou K, "Active fault rupture propagation in alluvial deposits", Proceedings, 9th International Conference of the Hellenic Geologic Society, Athens, September, 2001 (in Greek)

Cole DA Jr and Lade PV, "Influence zones in Alluvium over Dip-Slip Faults", Journal of Geotechnical Engineering, ASCE, 110 (5), 599-615, 1984

Itasca Consulting Group, Inc, Minneapolis, "FLAC – Fast Lagrangian Analysis of Continua Version 3.4, User's Guide" 1998

Kelson KI, Kang K-H, Page WD, Lee C-T and Cluff LS, "Representative styles of deformation along the Chelungpu Fault from the 1999 Chi-Chi (Taiwan) Earthquake: Geomorphic Characteristics and Responses of Man-made structures", Bulleting of the Seismological Society of America, 91 (5), 930-952, 2001

Lade PV, Cole DA Jr, and Cummings D. "Multiple Failure Surfaces Over Dip-Slip Faults", Journal of Geotechnical Engineering ASCE, 110 (5), 616-627, 1984

Loukidis D, "Active fault rupture propagation through soil layer", Diploma Thesis, N.T.U.A. 1999 (in Greek)

Loukidis D and Bouckovalas GD, "Numerical simulation of active fault rupture propagation through dry soil", Proceedings, 4th International Conference on Recent Advances in Geotechnical Earthquake Engineering and Soil Dynamics Symposium in honor of Professor W. D. Liam Finn, San Diego, CA, March 26-31, Paper 3.04, 2001

Mercier J-L, Carey-Gailhardis E, Mouyaris N, Simeakis K, Rondoyanis T and Anghelidis C, "Structural analysis of recent and active faults and regional state of stress in the epicentral area of the 1978 Thessaloniki earthquakes (Northern Greece)", Tectonics, 2, 577-600, 1983

Raptakis D, Chavez-Garcia FJ, Makra K and Pitilakis K, "Site effects at Euroseistest-I: Determination of the valley structure and confrontation of observations with 1D analysis", Soil Dynamics and Earthquake Engineering, 19(1), 1-22, 2000

Roth WH, Scott RF and Austin I, "Centrifuge modeling of fault propagation through alluvial soils", Geophysical Research Letters, 8 (6), 561-564, 1981

Roth, WH, Kalsi G, Papastamatiou D and Cundall PA, "Numerical Modeling of Fault Propagation in Soil", Proceedings of the 4th International Conference on Numerical Methods in Geomechanics, Edmonton, Canada, 487-494, 1982